Biomedicine & Pharmacotherapy 168 (2023) 115829

Contents lists available at ScienceDirect

Biomedicine & Pharmacotherapy

journal homepage: www.elsevier.com/locate/biopha

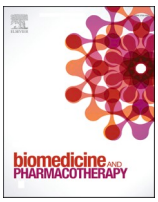

Multi-omics analysis of zebrafish response to tick saliva reveals biological processes associated with alpha-Gal syndrome

Rita Vaz-Rodrigues [a], Lorena Mazuecos [a], Margarita Villar [a,b], Marinela Contreras [a], Sara Artigas-Jerónimo [b], Almudena González-García [a], Christian Gortázar [a], José de la Fuente [a,c,*]

[a] SaBio, Instituto de Investigación en Recursos Cinegéticos IREC-CSIC-UCLM-JCCM, Ronda de Toledo 12, 13005 Ciudad Real, Spain
[b] Biochemistry Section, Faculty of Science and Chemical Technologies, University of Castilla-La Mancha, 13071 Ciudad Real, Spain
[c] Department of Veterinary Pathobiology, Centre for Veterinary Health Sciences, Oklahoma State University, Stillwater, OK 74078, USA

ARTICLE INFO

Keywords:
Alpha-Gal syndrome
Danio rerio
Multi-omics
Transcriptomics
Proteomics

ABSTRACT

The alpha-Gal syndrome (AGS) is a tick-borne allergy. A multi-omics approach was used to determine the effect of tick saliva and mammalian meat consumption on zebrafish gut transcriptome and proteome. Bioinformatics analysis using R software was focused on significant biological and metabolic pathway changes associated with AGS. Ortholog mapping identified highly concordant human ortholog genes for the detection of disease-enriched pathways. Tick saliva treatment increased zebrafish mortality, incidence of hemorrhagic type allergic reactions and changes in behavior and feeding patterns. Transcriptomics analysis showed downregulation of biological and metabolic pathways correlated with anti-alpha-Gal IgE and allergic reactions to tick saliva affecting blood circulation, cardiac and vascular smooth muscle contraction, behavior and sensory perception. Disease enrichment analysis revealed downregulated orthologous genes associated with human disorders affecting nervous, musculoskeletal, and cardiovascular systems. Proteomics analysis revealed suppression of pathways associated with immune system production of reactive oxygen species and cardiac muscle contraction. Underrepresented proteins were mainly linked to nervous and metabolic human disorders. Multi-omics data revealed inhibition of pathways associated with adrenergic signaling in cardiomyocytes, and heart and muscle contraction. Results identify tick saliva-related biological pathways supporting multisystemic organ involvement and linking α-Gal sensitization with other illnesses for the identification of potential disease biomarkers.

1. Introduction

Ticks are obligate hematophagous ectoparasites responsible for the transmission of a wide range of infectious agents [1,2]. Additionally, the inoculation of tick saliva into the host body is capable of modulating their immune response, occasionally leading to the development of tick-borne allergies such as the alpha-Gal syndrome (AGS) [3,4]. The AGS is a pathognomonic immunoglobulin E (IgE)-mediated delayed anaphylaxis that occurs 2–6 h after consumption of mammalian meat like pork, beef or lamb [5–7]. The reaction is triggered by the oligosaccharide galactose-alpha-1,3-galactose (α-Gal), found in both glycoproteins and glycolipids from non-catarrhine mammalian muscle cells and secretions [8,9]. As Old-World monkeys, apes and humans evolved with the inability to synthesize α-Gal epitopes, producing natural anti-α-Gal antibodies when exposed to this moiety, normally in response to gut bacteria or pathogen infection [10,11]. In AGS, sensitization to IgE initially occurs from hard-body tick bites due to tick salivary α-Gal-containing glycoproteins and glycolipids (Román-Carrasco et al., 2019; 2021; Chakrapani et al., 2022), but it has also been recently associated to other biomolecules such as prostaglandin E2 (PGE2) [12,13]. Although the mechanisms behind tick-induced sensitization to α-Gal remain unclear, tick sialome components may play a significant role in triggering the immune response cascade [14,15]. Despite being considered an emerging life-threatening allergy, not all individuals bitten by ticks and carrying elevated specific IgE (sIgE) against α-Gal develop AGS [5,16]. Moreover, symptomatology is extremely variable and individual-specific, ranging from a delayed anaphylactic reaction to gut related symptoms (abdominal pain, emesis and diarrhea), cutaneous (delayed pruritus, urticaria and angioedema) and respiratory (dyspnea and hypoxia) signs [17–20]. A minority of patients also reported cardiovascular changes and a possible link between α-Gal sensitization and coronary artery disease (CAD) [20–22]. Furthermore, a recent case

* Corresponding author at: SaBio, Instituto de Investigación en Recursos Cinegéticos IREC-CSIC-UCLM-JCCM, Ronda de Toledo 12, 13005 Ciudad Real, Spain.
E-mail addresses: jose_delafuente@yahoo.com, josedejesus.fuente@uclm.es (J. de la Fuente).

https://doi.org/10.1016/j.biopha.2023.115829
Received 30 August 2023; Received in revised form 17 October 2023; Accepted 31 October 2023
Available online 2 November 2023

report highlighted atypical neuro-psychiatric manifestations in a sensitized α-Gal individual [23].

In biomedical research, the application of zebrafish (*Danio rerio*) as an animal model in the study of human diseases is experiencing a rapid and supported expansion [24,25]. Due to the anatomical, genetic and physiological homology with humans, zebrafish have been implemented mostly in toxicological, behavioral, pharmacological, oncological and genetic studies [24,26]. Nevertheless, this small fresh-water teleost also represents a relevant model to study inflammatory diseases of the respiratory system [27,28] and, it holds potential for studying allergic reactions and immune mechanisms triggered by tick salivary biogenic substances and mammalian meat consumption [29–31]. Association of next-generation sequencing and shotgun proteomics data with disease modeling in zebrafish is accelerating the understanding of molecular mechanisms and defects associated with a particular experimental condition or human disease [32–34]. Moreover, integration of transcriptomics and proteomics data analysis enables a network-based study that unravels the intricate nature and functionality of biological systems [34,35]. This approach can uncover important effectors within signaling pathways and contribute to the discovery of novel biotargets, enhancing efforts in disease diagnose, prevention and control [32,35].

In this study, we used a multi-omics approach to determine the effect on the transcriptome and proteome gut profiles of zebrafish inoculated with tick saliva followed by mammalian meat consumption. Through bioinformatic analysis, we sought for significant biological and metabolic pathway changes, in order to fill up some of the current knowledge gaps associated with the AGS. In addition, ortholog mapping allowed to obtain highly concordant biological 1:1 human ortholog genes for the detection of gene-disease associations (GDAs) and disease enriched pathways. This experimental approach can provide valuable insights on the underlying pathomechanisms of AGS, enabling the identification of key genes and proteins that may serve as potential disease biomarkers.

2. Materials and methods

2.1. Animals and study design

The experiment was designed to characterize zebrafish response to tick saliva associated with allergic reactions to mammalian meat consumption and AGS (Fig. 1A) [29–31]. Saliva was collected from semi-engorged, pathogen-free, α-Gal-containing *Ixodes ricinus* female ticks [31,36]. Phosphate-buffered saline (PBS) was used as negative control. Wild type adult (6–8-month-old) AB strain zebrafish (10 animals per group; 1:1 female to male ratio; 033 ± 0.07 g) were provided by Dr. Juan Galcerán Sáez from the Instituto de Neurociencias (IN-CSIC-UMH, Sant Joan d'Alacant, Alicante, Spain) and certified by Biosait Europe S.L. (Barcelona, Spain; https://biosait.com) as free of major fish pathogens [29]. Zebrafish were maintained in a flow-through water system at 27 °C with a light/dark cycle of 14 h/10 h and fed twice

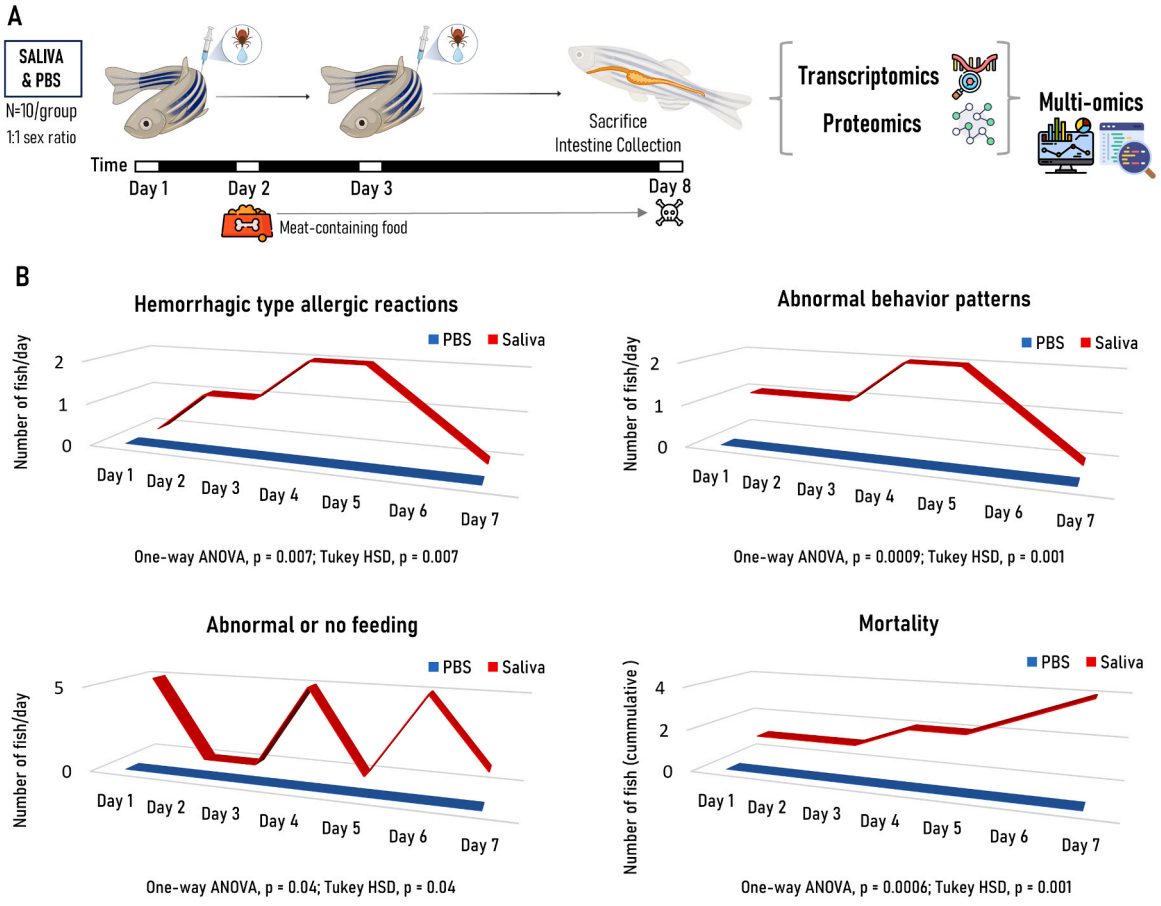

Fig. 1. Experimental design and characterization of allergic reactions to tick saliva and mammalian meat consumption in the zebrafish model. (A) Zebrafish were intramuscularly inoculated with *Ixodes ricinus* tick saliva or PBS as negative control. Wild type adult AB strain zebrafish (10 animals/group; 1:1 female to male ratio) were kept on fish feed during pre-treatment and until Day 2. Zebrafish were injected with each treatment at Days 0 and 3, and from Day 2 and until the end of the experiment at Day 8 fish were fed with dog food containing mammalian meat. After fish euthanasia, intestine tissue samples were collected and used for transcriptomics and proteomics analyses with multi-omics integration of obtained datasets. (B) Zebrafish hemorrhagic type allergic reactions, abnormal behavior patterns, abnormal or no feeding and accumulated mortality were examined from Day 1 and followed daily until the end of the experiment at Day 8. Results were compared between treatments by one-way ANOVA test with post-hoc Tukey HSD test ($p \leq 0.05$; N = 6–10 biological replicates).

daily at 9:30 am and 1:30 pm with dry fish feed (Premium food tropical fish, DAPC, Valladolid, Spain; 50–70 μg/fish) during pre-treatment and until Day 2. Following previously described procedures [31,37], at Days 0 and 3, zebrafish were subcutaneously injected with each treatment (1 μL tick saliva plus 9 μL PBS or 10 μL PBS) by inserting the needle 2 mm underneath the skin holding the syringe at an angle of 15–20 deg to the horizontal plane near the zebrafish tail. From Day 2 and until the end of the experiment at Day 8 fish were fed with dog food containing mammalian meat (Classic red, ACANA, Champion Petfoods LP, Edmonton, Canada; 150–200 μg/fish) [29]. Zebrafish hemorrhagic type allergic reactions (skin redness and hemorrhagic anaphylactic-type reactions appearing 3–5 h posttreatment with hemorrhage affecting various organs), abnormal behavior and feeding patterns (no feeding, low mobility, standing motionless at the bottom of the water tank, and zigzag-type swimming) and accumulated mortality were examined throughout the experiment and compared between groups to access the effect of treatments and dog food after feed change and treatment between Days 1 and 7, as previously reported [29]. Representative images and movies for hemorrhagic type allergic reactions and abnormal behavior and feeding patterns can be found at Contreras et al. [29,30]. These parameters were compared between treatments by one-way ANOVA test with post-hoc Tukey HSD test using the freely available online web calculator Astatsa [38] and a p value < 0.05 for statistical significance. Zebrafish were euthanized at Day 8 by immersion in 0.4% tricaine methanesulfonate (MS-222) and subsequently placed on ice [39,40]. The ELISA for anti-α-Gal IgM antibody titers in zebrafish was conducted as previously described [31] and results compared by one-way ANOVA test with post-hoc Tukey HSD test ($p < 0.05$). Intestine tissue samples were collected from each individual and used to extract mRNA and proteins for transcriptomics and proteomics analyses with multi-omics integration of obtained datasets.

2.3. Transcriptome: total mRNA extraction and sequencing analysis

Zebrafish intestinal tissue samples collected during fish necropsy were used to extract mRNA. Firstly, up to 30 mg of tissue per sample was disrupted with a scalpel and homogenized with a tissue grinder until lysates were completely clear. Total mRNA was isolated from 15 samples using the AllPrep DNA/RNA/Protein Mini Kit (Qiagen, Hilden, Germany) and following manufacturer's instructions. For tick saliva group, the 6 independent biological samples were pooled in pairs, while the other 9 PBS control samples were pooled in groups of three.

Library preparation and sequencing were conducted in Seqplexing (Valencia, Spain). Briefly, around 18.4–49.3 million (M) of total reads were generated from each library for the RNA sequencing (RNA-Seq) data. The Read 1 and Read 2 FASTQ files were analysed by FastQC (0.11.5) [42] and primary quality control (QC) was performed. The UMI reads were identified, and adapter and poly A/T sequences were trimmed by using UMI-tools (1.1.2) [43] and Cutadapt (3.7) [44]. The STAR (2.7.3) [45] aligner was used to align reads to the *Danio rerio* reference genome (GRCz11.107). After alignment, the final BAM files were deduplicated with UMI-tools and quantified with *featureCounts* function available in Bioconductor R package *Rsubread* [46] by GRCz11.107 annotations.

After mapping, we filtered out lowly expressed genes from the provided table of raw count units based on a minimum of 5 counts per sample and with a minimum sum threshold of 50 counts per gene across all samples. Due to technical issues, we cautiously excluded one outlying sample from each group in order to prevent skewing of the overall analysis. To perform differential expression analysis for sequence data (DESeq) we used Bioconductor (version 3.16) *DESeq2* package [47] from R software, version 4.2.3 [48]. This fits the normalized count data in a negative binomial generalized linear model to analyse differences between the conditions of interest (Tick Saliva versus PBS) and allows to extract the differentially expressed genes (DEGs) based on a Benjamini-Hochberg (BH) adjusted p-value cutoff < 0.05, a Log_2 Fold Change (logFC) $\geq |2|$ and an average overall expression level (base mean) > 50 (Supplementary Data 1, Sheets 1&2). Heatmap creation of the DEGs was performed using the *ComplexHeatmap* package [49] and the *Heatmap* function from R [48], combining data from normalized Z-score values (Z-score), logFC and base mean (AveExpr). The volcano plot highlighting DEGs of interest was created using the *EnhancedVolcano* package [50].

2.4. Proteome: protein extraction, digestion, and mass spectrometry analysis

Total protein from zebrafish intestine tissue samples was extracted using the AllPrep DNA/RNA/Protein Mini Kit (Qiagen). A total of 15 intestine protein extracts from individual zebrafish were clustered into 3 biological pools/group with 2–3 samples/pool. Protein concentration was measured with the BCA Protein Assay with BSA (Sigma-Aldrich) as standard. Afterwards, protein samples (200 μg/sample) were trypsin digested using the FASP Protein Digestion Kit (Expedeon Ltd., Cambridge, UK) and sequencing grade trypsin (Promega, Madison, USA), following manufacturer's instructions. The resulting tryptic peptides were then desalted onto OMIX Pipette tips C18 (Agilent Technologies, Santa Clara, USA), dried down and stored at − 20 °C until further mass spectrometry analysis.

The desalted protein digests were resuspended in 2% acetonitrile and 5% acetic acid in water and analysed by reverse-phase liquid chromatography mass spectrometry (RP-LC-MS/MS) using an Ekspert™ nanoLC 415 system coupled online with a 6600 TripleTOF mass spectrometer (AB SCIEX, Framingham, USA) through Information-Dependent Acquisition (IDA), followed by Sequential Windowed data independent Acquisition of the Total High-resolution Mass Spectra (SWATH-MS) [51].

To create a spectral library of all the detectable peptides in the samples, the IDA MS raw files were combined and subjected to database search in unison using ProteinPilot software v. 5.0.1 (AB SCIEX) with the Paragon algorithm. Spectra identification was performed by searching against the UniProt *Danio rerio* (zebrafish) proteome database (https://www.uniprot.org) (46,695 entries in July 2023) with the following parameters: iodoacetamide cysteine alkylation, trypsin digestion, identification focus on biological modification and thorough ID as search effort. The detected protein threshold was set at 0.05. An independent False Discovery Rate (FDR) analysis, using the target–decoy approach provided by Protein Pilot was performed to assess the quality of identifications. Positive identifications were considered when identified proteins reached 1% of global FDR.

For SWATH processing, up to 10 peptides with 7 transitions/protein were automatically selected by the SWATH Acquisition MicroApp 2.0 in the PeakView 2.2 software with the following parameters: 15 ppm ion library tolerance, 5 min XIC extraction window, 0.01 Da XIC width, and considering only peptides with at least 99% confidence (excluding either shared or modified ones). To ensure reliable quantitation, only proteins with three or more peptides available for quantitation were selected for XIC peak area extraction and exported for analysis in the MarkerView 1.3 software (AB SCIEX). Global normalization was conducted according to the Total Area Sums (TAS) of all detected proteins in samples. A Student's t test ($p \leq 0.05$) was then used to perform two-sample comparisons between the averaged TAS of all the transitions derived from each protein across the 3 replicate runs/group to identify significantly differentially represented proteins (DRPs) between groups (Supplementary Data 2, Sheets 1&2). Heatmap creation of the DRPs was performed using the *ComplexHeatmap* package [49] and the *Heatmap* function from R [48], combining data from Z-score and logFC.

2.5. Functional annotation and enrichment analysis

To obtain the functional prolife of significant transcript and protein sets, the gene ontology (GO) biological process (BP) database was used

at GO distribution level 3 with the *groupGO* function from the R package *clusterProfiler* [48,52,53]. The gene set enrichment analysis (GSEA) was performed using the GO BP database with the *gseGO* function from *clusterProfiler* package [52–54], utilizing 10 000 permutations and a BH adjusted p-value cutoff of 0.01 for the transcriptome and 0.05 for the proteome, in order to pinpoint significant pathways. Moreover, the Kyoto Encyclopedia of Genes and Genomes (KEGG) GSEA analysis was carried out with *gseKEGG* function from package *clusterProfiler* [52–54], employing 10 000 permutations and a BH adjusted p-value lower than 0.05 for both transcriptomics and proteomics data, to identify significant biochemical pathways. Annotation data of the zebrafish (*Danio rerio*) genome was obtained from the mapping library of R package *org.Dr.eg.db* [55]. The R package *enrichplot* [56] was used for visual representation of the functional enrichment results.

2.6. Ortholog mapping, gene-disease associations (GDAs) and disease enriched pathways

For transcriptome and proteome ortholog mapping the *convert_othologs* function from the *orthogene* package [57] was employed with the *gprofiler* method and the *drop_both_species* feature that allowed to obtain highly concordant biological 1:1 orthologs genes between zebrafish (*Danio rerio* – input species) and human (*Homo sapiens* – output species).

Retrieving gene-disease associations (GDAs) using MeSH terms in DisGeNET platform from human orthologs was carried out with the *gene2disease* function from the *disgenet2r* R package [48,58]. To perform enrichment analysis (Fisher test) over the diseases in DisGeNET for transcript and protein data, the *disease_enrichment* function from the previously mentioned package was applied with a FDR ≤ 0.05. All of these analyzes included data from following curated databases: Comparative Toxicogenomics Database (CTD), Psychiatric disorders Gene association NETwork (PsyGeNET), Human Phenotype Ontology (HPO), Genomics England PanelApp, Clinical Genome Resource (ClinGen), Cancer Genome Interpreter (CGI), UniProt and Orphanet.

2.7. Multi-omics approach

The *mutiGSEA* R package [48,59] was used to run a robust GSEA-based pathway enrichment for the omics layers of transcriptomics and proteomics. The enrichment was calculated with the *multiGSEA* function for each omics layer separately and aggregated p-values were calculated afterwards with the Stouffers Z-method to derive a composite multi-omics pathway enrichment. Features at transcriptome level were mapped using the Ensembl ID format, meanwhile proteome was mapped with UniProt IDs. Pathway enrichment values for each omics layer were obtained as well as aggregated pathway enrichment scores of Reactome, KEGG and WikiPathways zebrafish databases (Supplementary Data 3).

2.8. Reverse transcriptase quantitative PCR (RT-qPCR)

To confirm validity of transcriptomics results, RT-qPCR was performed on target DEGs utilizing the CFX96 real-time PCR detection system (Bio-Rad, Hercules, USA). PCR conditions comprised a reverse transcription reaction at 50 °C for 10 min, followed by an initial denaturation step at 95 °C for 1 min, amplification by 40 cycles of 95 °C for 20 s and 60 °C for 1 min, followed by a dissociation curve analysis. For a total volume of 20 μL, the PCR mixture contained 1.5 μL (150 ng) of sample mRNA, 10 μL of SYBR Green Master Mix (Bio-Rad), 0.25 μL of iScript reverse transcriptase, 1 μL (10 μM) of forward and reverse primers (Sigma-Aldrich) each and 6.25 μL of nuclease-free water. Each PCR reaction had 3 technical replicates/sample and 2 negative controls. Primers used were designed with primer-BLAST tool [60] and are listed in Supplementary Table 1. The generalized qBase model was employed to normalize the expression of the target DEGs [61,62]. This method employs gene specific PCR efficiency correction and the geometric averaging of selected housekeeping genes (β-*actin 1* [*actb1*] and *glyceraldehyde 3-phosphate dehydrogenase* [*gapdh*]) in order to obtain calibrated, normalized and relative expression values. Furthermore, non-parametric Mann Whitney U test in R software, version 4.2.3, was used for statistical comparisons between groups [48].

2.9. Western blot analysis

Western blotting was conducted using antibodies against target DRPs actin alpha 2 (acta2), 60 kDa chaperonin (hspd1) and the loading control β-tubulin. Thirty micrograms of total protein per pooled sample was mixed with 2x Laemmli sample buffer (Bio-Rad) containing β-mercaptoethanol (βME) and run on a 12% SDS-PAGE precast gel (GenScript, Oxford, UK). Afterwards, proteins were transferred onto 0,45 μM nitrocellulose membranes, blocked with 5% skim milk in TBS 1% (blocking solution) for 1h30 at room temperature (RT), and washed 3 times (5 min each) with TBS 1% with 0.05% Tween 20 (TBS-T). Membranes were incubated overnight on a shaker at 4 °C with rabbit anti-acta2 (1:2000 dilution, polyclonal, Thermo Fisher PA5–85070), anti-hspd1 (1:1000 dilution, monoclonal, Cell Signaling Technology #12165) or anti-β-tubulin (1:3000 dilution, polyclonal, Thermo Fisher PA5–98221) antibodies. After being washed with TBS-T solution 3 times, the nitrocellulose membranes were incubated with a goat anti-rabbit polyclonal IgG conjugated with horseradish peroxidase (HRP, 1:1000 dilution in blocking solution, Sigma-Aldrich) on a shaker for 1 h 30 min at RT. The membranes were then washed 3 times with TBS-T and treated with Pierce ECL Western Blotting Substrate (Thermo Fisher) in order to visualize results. ImageJ software was used to quantify representation of target DRPs and loading control. DRPs levels were normalized against the loading control and graphically compared between groups using GraphPad Prism, version 8.0.1.

3. Results

3.1. Characterization of allergic reactions in response to tick saliva and mammalian meat consumption in the zebrafish model

Treatment with tick saliva resulted in increased mortality and significant higher incidence of hemorrhagic type allergic reactions, abnormal behavior and feeding patterns when compared to PBS-treated control ($p < 0.05$; Fig. 1B). The anti-α-Gal IgM antibody titers were significantly higher in zebrafish treated with tick saliva ($O.D._{450\ nm} = 0.63 \pm 0.09$) when compared to PBS-treated controls ($O.D._{450\ nm} = 0.22 \pm 0.05$) ($p < 0.05$; $n = 6–10$ biological replicates).

3.2. Transcriptomics

3.2.1. Differential expression, functional annotation and enrichment analysis

After subjecting 32 520 raw gene counts to DeSeq analysis and implementing various filtering steps as showcased in Fig. 2B, a total of 382 differentially expressed genes (DEGs), 114 upregulated and 268 downregulated, were identified (Supplementary Data 1, Sheets 1&2) and visually represented by means of a heatmap (Fig. 2A) and a volcano plot (Fig. 2C).

The upregulation of the *histidine triad nucleotide binding protein 1* (*hint1*) gene combined with the downregulation of gene *GATA binding protein 2a* (*gata2a*) and proto-oncogenes *junD* and *junE* suggests mast cell activation [63–65]. Furthermore, downregulated genes *early growth response 2a* (*egr2a)* and *calmodulin 1b (calm1b)* are associated with the innate immune pathway of c-type lectin receptor signaling [66].

Initial data exploration begun with the analysis of DEG-related GO BP pathways, leading to the identification of 88 upregulated and 116 downregulated pathways (Supplementary Data 1, Sheets 3&4). Subsequently, the GSEA method for GO BP yielded a total of 208 significantly enriched pathways (34 upregulated and 174 downregulated)

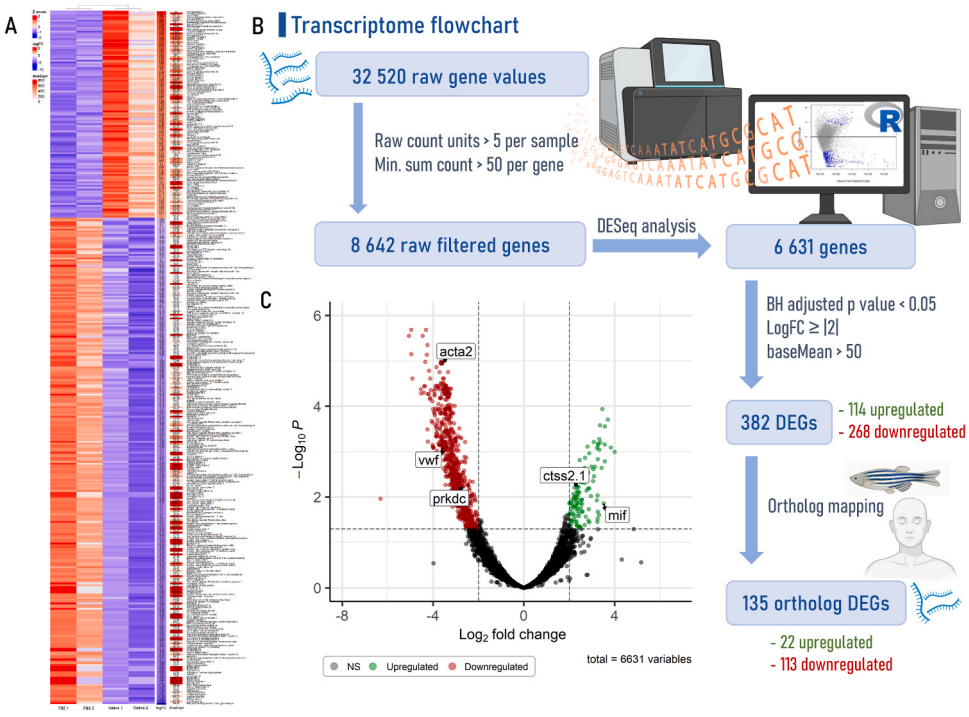

Fig. 2. Transcriptome pipeline and visual representation of gene expression from gut zebrafish underlying the effects of tick saliva followed by mammalian meat consumption. (A) Heatmap with the differentially expressed genes (DEGs) created using the *ComplexHeatmap* package and the *Heatmap* function from R software, version 4.2.3, combining data from normalized Z-score values (Z-score), log2FoldChange (logFC) and average overall expression level (baseMean or AveExpr). (B) Flowchart that leads to the acquisition of DEGs and ortholog DEGs. First step includes raw count units based on a minimum of 5 counts/sample and a minimum sum threshold of 50 counts/gene across all samples. Second step is the differential expression analysis for sequence data (DESeq), performed with Bioconductor (version 3.16) DESeq2 package [47] from R. Third step allows to extract DEGs based on a Benjamini-Hochberg (BH) adjusted p-value cutoff < 0.05, a logFC $\geq |2|$ and a baseMean > 50. Last step is ortholog mapping that utilizes the *convert_othologs* function from the *orthogene* package employed with the *gprofiler* method and the *drop_both_species* feature, allowing to obtain highly concordant biological 1:1 orthologs genes between zebrafish (*Danio rerio* – input species) and human (*Homo sapiens* – output species). (C) Volcano plot, highlighting DEGs of interest, created with the *EnhancedVolcano* package. *acta2: smooth muscle alpha-actin; ctss2.1: cathepsin S; mif: macrophage migration inhibitory factor; prkdc: DNA-dependent protein kinase; vwf: von Willebrand factor.*

(Supplementary Fig. 1; Supplementary Data 1, Sheet 5). Activated pathways were mostly related to reproductive processes, particularly acrosome reaction associated with fertility mechanisms involving sperm-egg recognition and binding [67]. Meanwhile, suppressed pathways were essentially associated with cardiac and skeletal muscle contraction, blood circulation, GTPase activity, sensory perception, neuronal morphogenesis and axon guidance in response to an external stimulus. Enriched pathways correlated with anti-Gal IgE and allergic reactions to tick saliva included downregulated pathways such as circulatory system process, blood circulation, heart contraction, behavior, sensory perception, detection and response to external stimulus [68–71]. On the other hand, GSEA KEGG analysis revealed 31 enriched pathways (Fig. 3A; Supplementary Data 1, Sheet 6), consisting of 8 activated pathways primarily related to oxidative phosphorylation, ribosome and proteasome, and 23 suppressed pathways mainly associated with the glutathione metabolism, actin adhesion and cardiac muscle contraction. In this case, significant downregulated tick saliva allergy-related pathways were cardiac and vascular smooth muscle contraction and adrenergic signaling in cardiomyocytes [20,71].

3.2.2. Ortholog mapping and disease ontology

Out of 382 zebrafish DEGs obtained, 135 highly concordant human orthologous genes, which corresponds to 35% of total DEGs (Supplementary Data 1, Sheet 7). Among the mapped genes, 22 were found to be upregulated and, within that group, 14 were linked to 91 human associations of a gene with a particular disease (GDAs) (Supplementary Data 1, Sheet 8). Associations observed were mostly related to disorders affecting the skin and connective tissue, immune and digestive systems (Fig. 3B). The DisGeNET enrichment revealed 9 significant associations with diseases such as spondyloenchondrodysplasia, osteogenesis imperfecta, mitochondrial complex I deficiency, ataxia-telangiectasia-like disorder, systemic juvenile idiopathic arthritis and squamous cell carcinoma of the head and neck (Supplementary Data 1, Sheet 9). Remarkably, these diseases are connected to the immune system, musculoskeletal system, nervous system, skin, and connective tissue or represent a nutritional/metabolic disease.

In regard to the 113 downregulated genes, 70 presented a total of 727 human GDAs (Supplementary Data 1, Sheet 10), particularly linked with the nervous, digestive and cardiovascular systems (Fig. 3B). The DisGeNET enrichment allowed to pinpoint 167 significant diseases type (Supplementary Data 1, Sheet 11) and 27% belonged to the nervous system (e.g., neurodevelopment disorders, epileptic encephalopathy and episodic ataxia), 17% to the musculoskeletal system (e.g., several myopathies and muscular dystrophies) and 12% to the cardiovascular system (e.g., acute coronary syndrome and several cardiomyopathies).

3.3. Proteomics

3.3.1. Differential representation, functional annotation and enrichment analysis

The SWATH-MS proteomics analysis allowed to identify a total of 955 proteins of which 182 were differentially represented (Supplementary Data 2, Sheets 1&2). Among the differentially represented proteins (DRPs), 7 were overrepresented while 175 were underrepresented. Results were visually depicted through a heatmap (Fig. 4A). Zebrafish mast cell-specific marker carboxypeptidase A5 (*cpa5*) was underrepresented in tick saliva group, as well as the innate immune related protein calmodulin [65,66].

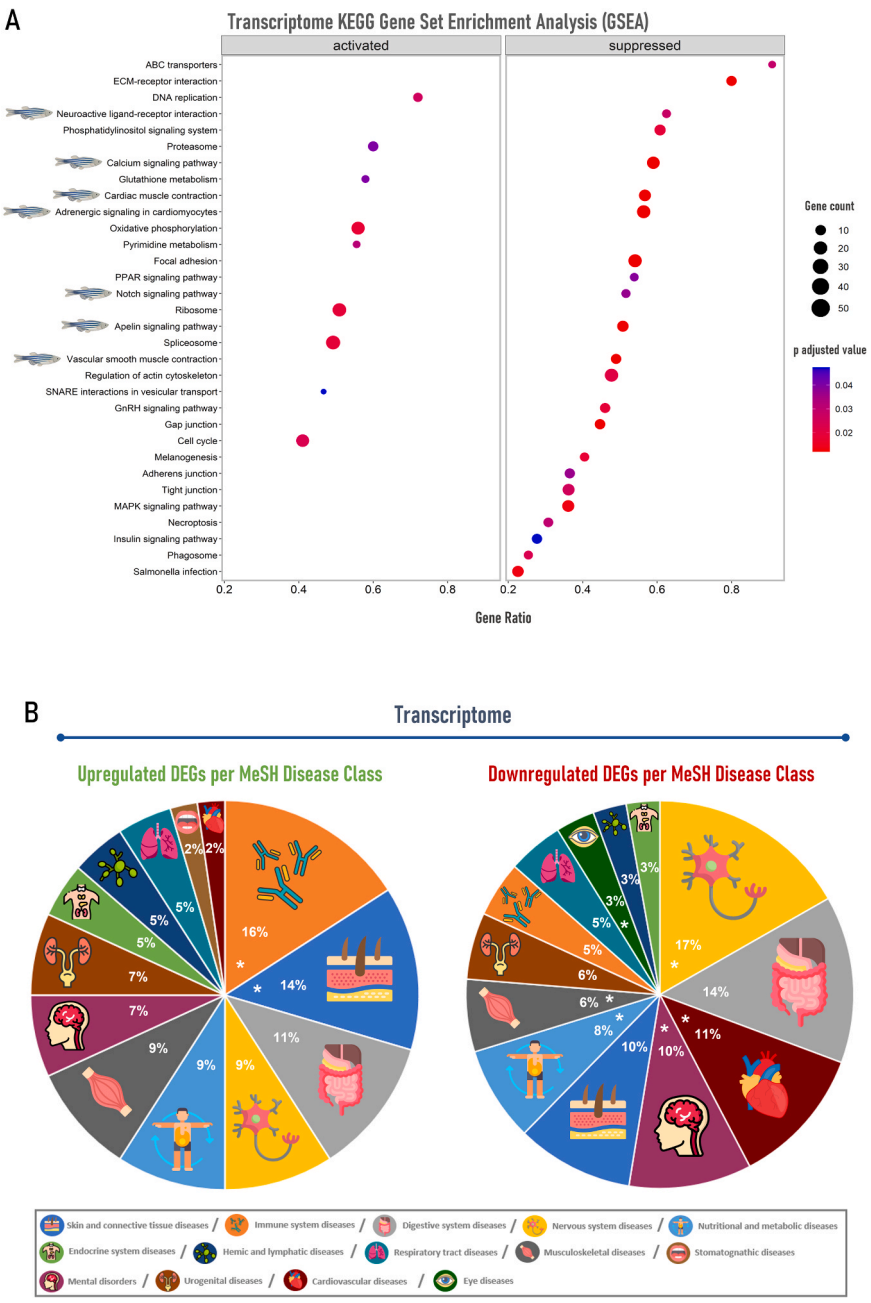

Fig. 3. Gut transcriptome enrichment analysis and orthologs gene-disease class associations of zebrafish inoculated with tick saliva followed by mammalian meat consumption. (A) Gene set enrichment analysis (GSEA) using the Kyoto Encyclopedia of Genes and Genomes (KEGG) database was carried out with *gseKEGG* function from package *clusterProfiler*, employing 10 000 permutations and a Benjamini-Hochberg (BH) adjusted p-value lower than 0.05. The dotplot was created with the R package *enrichplot* and each downregulated pathway related to tick saliva allergy is pointed out with a zebrafish illustration. (B) Upregulated and downregulated ortholog differentially expressed genes (DEGs) represented by disease class using MeSH terms in DisGeNET platform. Disease class groups are marked with an asterisk (*) when DisGeNET enrichment analysis showed ≥ 4 significant diseases/class group in the upregulated gene set and ≥ 10 diseases/class group in the downregulated gene set.

Initial analysis of DRP-related GO BP pathways revealed the identification of 13 overrepresented and 106 underrepresented pathways (Supplementary Data 2, Sheets 3&4). Afterwards, the GSEA method for GO BP yielded a total of 47 significantly enriched pathways (14 overrepresented and 33 underrepresented) (Fig. 4B; Supplementary Data 2, Sheet 5). Activated pathways show several overlapping gene sets related to cellular response to a stimulus, in this case, estrogen but also negative regulation of gene expression. In other hand, suppressed pathways are mostly related with lipids biosynthesis and regulation of the glucose metabolism. There are also suppressed vias associated with the production of reactive oxygen species (ROS), a process known to be modulated by tick saliva in the host immune system response [1]. Furthermore, GSEA KEGG analysis revealed only 5 significant suppressed pathways (Fig. 4C; Supplementary Data 2, Sheet 6), some associated with fatty acid metabolic routes such as PPAR signaling pathway and others with ribosomal pathways or even inhibition of cardiac muscle contraction.

3.3.2. *Ortholog mapping and disease ontology*

From the 182 zebrafish DRPs, 119 highly concordant human orthologs genes were identified by using the Ensemble Prot ID, yielding a total mapping of 66% (Supplementary Data 2, Sheet 7). Out of the results

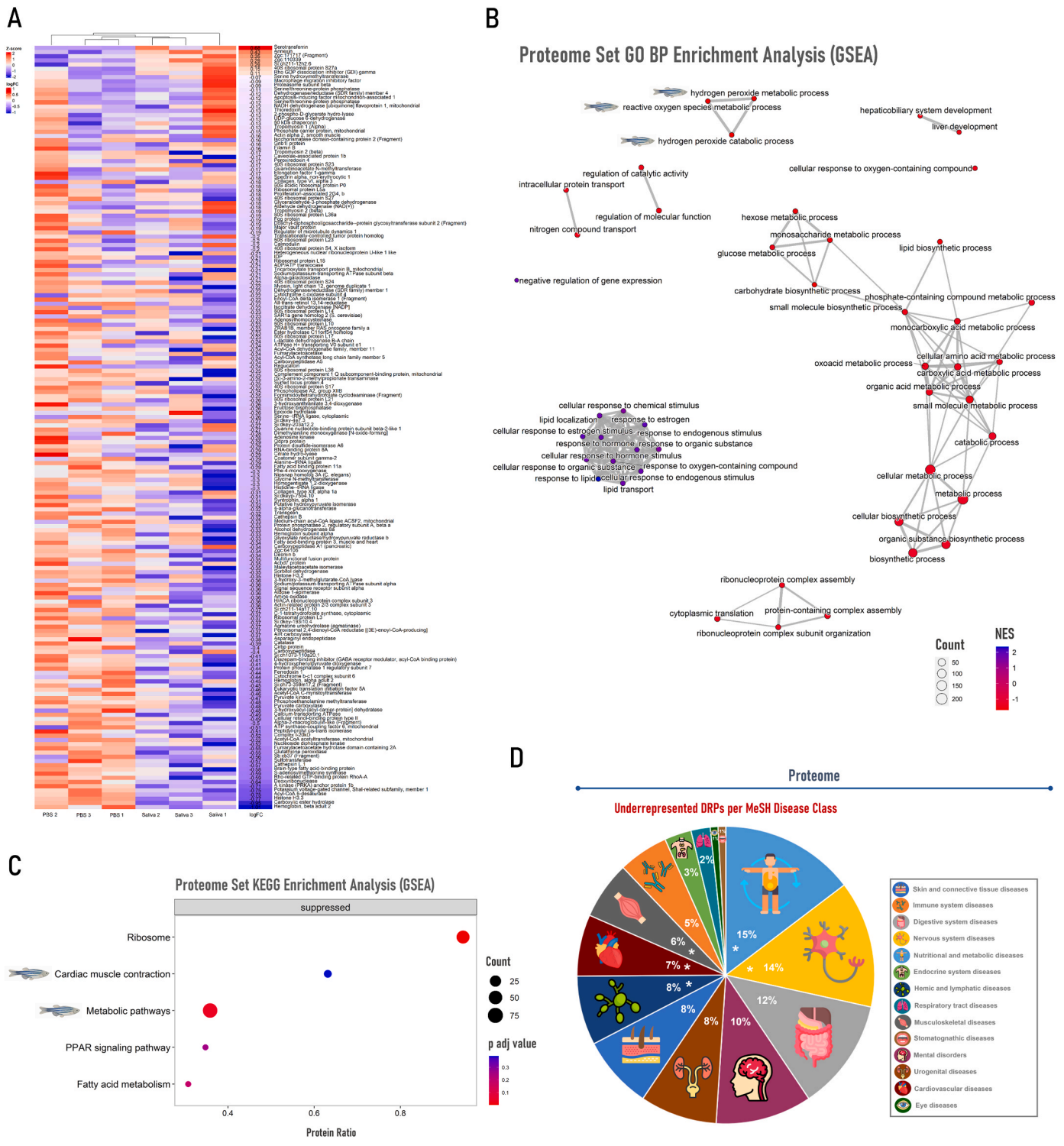

Fig. 4. Gut proteome heatmap, enrichment analysis and orthologs disease class associations of zebrafish inoculated with tick saliva followed by mammalian meat consumption. (A) Heatmap of differentially represented proteins (DRPs), combining data from normalized Z-score values (Z-score) of pooled samples and logFoldChange (logFC). Heatmap creation was performed with the *ComplexHeatmap* package and the *Heatmap* function from R software, version 4.2.3. (B) Proteome biological process (BP) enrichment analysis (GSEA method) was executed with the *gseGO* function from *clusterProfiler* package, utilizing 10 000 permutations and a Benjamini-Hochberg (BH) adjusted p-value lower than 0.05. This emapplot was created with the R package *enrichplot* and each downregulated pathway related to tick saliva allergy is highlighted with a zebrafish illustration. (C) Proteome enrichment analysis (GSEA method) using the Kyoto Encyclopedia of Genes and Genomes (KEGG) database was carried out with *gseKEGG* function from package *clusterProfiler*, employing 10 000 permutations and a BH adjusted p-value lower than 0.05. The dotplot was created with the R package *enrichplot* and each downregulated pathway related to tick saliva allergy is emphasized with a zebrafish illustration. (D) Underrepresented DRPs characterized by disease class using MeSH terms from the DisGeNET platform. Disease Class Groups are marked with "* " when DiGeNET enrichment analysis showed $\geq$ 10 diseases/class group in the underrepresented protein set. NES: Normalized Enriched Score.

obtained, only 2 genes belonged to overrepresented proteins. One of the proteins identified was melanotransferrin (orthologous of zebrafish serotransferrin), that possessed 1 gene disease association related to the development of melanoma (Supplementary Data 2, Sheet 8), using the same filtering settings as previously mentioned for transcriptomics data. Interestingly, this was the only pathway significantly enriched (FDR = 0.026) in the DisGeNET analysis.

Regarding the 117 underrepresented proteins, it was found that 87 of them exhibited a total of 801 GDAs (Supplementary Data 2, Sheet 8) that were predominantly categorized as nutritional and metabolic, nervous, or digestive systems diseases (Fig. 4D). The DisGeNET enrichment analysis revealed 160 significant diseases related to the underrepresented proteins (Supplementary Data 2, Sheet 9), with 31% linked to the nervous system and 27% related with nutritional and metabolic disorders. Diseases such as phenylketonuria, hyperphenylalaninemia and pyruvate carboxylase deficiency are connected to both systems.

3.4. Multi-omics approach

Merging of transcriptomics (DEGs) and proteomics (DRPs) datasets allowed to pinpoint 12 genes/proteins, of which 4 belonged to upregulated genes and 8 to downregulated ones. The overexpressed genes encoded 3 novel proteins (zgc:171717 [fragment], zgc:110339 and si:ch211–12h2.6) that were overrepresented as well, but also the macrophage migration inhibitory factor (mif) that gave rise to an underrepresented protein. Moreover, underexpressed genes all turned out to encode underrepresented proteins (Table 1).

Furthermore, multi-omics pathway enrichment of transcriptomics and proteomics layers employing Reactome, KEGG and WikiPathways zebrafish databases revealed 53 enriched pathways at mRNA level and 78 at protein level but only 3 significant pathways when analysing aggregated adjusted p-values (Supplementary Data 3). Enriched integrated pathways were all suppressed routes and had relation with adrenergic signaling in cardiomyocytes, cardiac muscle contraction (KEGG data) and muscle contraction (Reactome data).

3.5. Target selection and data validation

Target selection for validation of gene expression and protein representation was based on the biological importance of the DEGs/DRPs of interest and its presence on both omics datasets. In this case, we focused on targets whose GO BP pathways and MeSH disease class were associated with AGS-related symptoms of hemorrhagic type allergic reactions, cardiovascular and gastrointestinal changes, abnormal behavior, mortality and immune response (Table 2) [4,20,29].

In order to validate expression results from RNA-seq data analysis, changes in mRNA levels of 5 target DEGs were quantified by RT-qPCR, including the 2 upregulated genes *macrophage migration inhibitory factor (mif)* and *cathepsin S (ctss2.1)*, and 3 downregulated ones, namely *DNA-dependent protein kinase* (*prkdc*), *von Willebrand factor (vwf)* and *smooth muscle alpha-actin (acta2)*. RT-qPCR results were consistent with RNA-seq analysis in 4 out of 5 DEGs, showcasing an 80% correlation of expression patterns (Fig. 5A). Reliability of proteomics data by Western blotting confirmed underrepresentation of target DRPs, actin alpha 2 (UniProt ID: Q6DHS1) and 60 kDa chaperonin (UniProt ID: Q803B0), in the treatment group (Fig. 5B; Supplementary Fig. 2). Results of analyzed targets are summarized in Fig. 5C.

4. Discussion

To the best of our knowledge, this is the first study that provides a multi-omics approach to determine the effect on the transcriptome and proteome gut profiles of zebrafish inoculated with tick saliva, followed by mammalian meat consumption. Transcriptomics analysis showed downregulation of biological and metabolic pathways associated with blood circulation, cardiac and vascular smooth muscle contraction, behavior, and sensory perception. Disease enrichment analysis revealed that downregulated orthologous genes were mostly associated with human disorders affecting the nervous, musculoskeletal, and cardiovascular systems. In other hand, proteomics analysis unveiled the suppression of pathways associated with the immune system production of reactive oxygen species (ROS) and cardiac muscle contraction. Furthermore, underrepresented proteins were mainly linked to nervous and nutritional/metabolic human disorders. Finally, multi-omics pathway enrichment showcased significant suppressed routes related to adrenergic signalling in cardiomyocytes, as well as heart and muscle contraction.

Almost 15 years have passed since the discovery of the AGS and yet this disease keeps surprising doctors and scientists due to its intertwining symptomatology and complex pathogenesis [5,6,72]. In this study, zebrafish injected with tick saliva showed increased mortality and significant higher incidence of hemorrhagic type allergic reactions, changes in behavior and feeding patterns. Our previous studies showed that only zebrafish fed with mammalian meat containing α-Gal displayed the observed symptoms, whereas those fed with α-Gal-free fish feed did not [29,31]. In humans, AGS mortality rates are unknown due to the higher number of underdiagnosed cases and unique presentation of delayed anaphylaxis [73]. Nevertheless, AGS is still considered a life-threatening illness with symptomatology ranging from cutaneous and gastrointestinal problems to less common respiratory, oropharyngeal, cardiovascular and nervous symptoms [4,20,23].

Disease modeling of AGS with zebrafish integrating transcriptomics and proteomics data analysis allowed for the discovery of biological and metabolic pathways that correlated with anti-Gal IgE and allergic

Table 1
Common differentially expressed genes (DEGs)/differentially represented proteins (DRPs) in merged transcriptomics and proteomics datasets.

NCBI ZF ID	Gene symbol	UniProt ID	Protein name	LogFC mRNA	LogFC protein	p value mRNA	p value protein
751093	mif	Q0ZBR7	Macrophage migration inhibitory factor	3.514	-0.086	0.0138	0.036
795141	zgc:171717	F1QA36	Zgc:171717 (fragment)	3.224	0.348	0.0008	0.025
550490	zgc:110339	F1RAM4	Zgc:110339	2.342	0.293	0.0416	0.039
562920	si:ch211–12h2.6	E7EZV4	Si:ch211–12h2.6	2.324	0.286	0.0152	0.028
559001	fasn	E7F5V3	3-Hydroxyacyl-[acyl-carrier-protein] dehydratase	-2.168	-0.484	0.0100	0.044
100149543	col12a1a	X1WF98	Collagen, type XII, alpha 1a	-3.258	-0.306	0.0001	0.005
393908	tpm1	Q6NYQ0	Tropomyosin 1 (alpha)	-3.259	-0.133	5.01E-05	0.003
768287	desmb	F1QK59	Desmin b	-3.303	-0.342	5.38E-05	0.005
415209	tpm2	A0A0R4IAL5	Tropomyosin 2 (beta)	-3.311	-0.185	5.38E-05	0.020
64267	atp1b1a	Q9DGL3	Sodium/potassium-transporting ATPase subunit beta	-3.356	-0.212	0.0009	0.003
100001681	kcnd1	B0UYF4	Potassium voltage-gated channel, Shal-related subfamily, member 1	-3.458	-0.749	0.0007	0.021
322509	acta2	Q6DHS1	Actin alpha 2, smooth muscle	-3.589	-0.155	1.09E-05	0.044

FC: Fold Change; ZF: zebrafish.

Table 2
Selected differentially expressed genes (DEGs) and/or differentially represented proteins (DRPs) functional annotation, enrichment analysis and disease ontology results.

Target	LogFC RNA	LogFC protein	GO terms – Biological Processes (level 3)	Enrichment analysis (BP & KEGG)	Disease class & enrichment analysis
Macrophage migration inhibitory factor (mif)	3.514	- 0.086	Cell death	Negative regulation of apoptotic processes	Related to all disease classes, mostly immune system diseases (e.g., rheumatoid arthritis)
Cathepsin S (ctss2.1)	2.410	absent	Immune response	Lysosome (NS)	Obesity and contact hypersensitivity
60 kDa chaperonin (hspd1)	1.3775 (NS)	-0.128	Leukocyte activation and migration, cytokine production, cell death and response to stress	RNA degradation (NS)	Nervous system and cardiovascular diseases (acute coronary syndrome and hypertrophic cardiomyopathy)
DNA-dependent protein kinase (prkdc)	-2.669	absent	Leukocyte activation and somatic diversification of immune receptors	Phosphorylation and intracellular signal transduction	Nervous system and immune system diseases (combined immunodeficiency)
Von Willebrand factor (vwf)	-3.583	absent	Coagulation and response to stress	Cell-substrate adhesion and ECM-receptor interaction	Hemic and lymphatic diseases, cardiovascular diseases (atrial fibrillation)
Smooth muscle alpha-actin (acta2)	-3.589	-0.155	Positive regulation of metabolic process, tissue migration and anatomical structure morphogenesis	Vascular smooth muscle contraction, heart contraction and apelin signalling pathway	Mostly neoplasms, cardiovascular (aortic aneurysm) and nervous system diseases (moyamoya disease)

FC: Fold Change; NS: not statistically significant.

reactions to tick saliva [31]. Zebrafish allergic response was driven by IgM production and mast cell activation through *hint1* upregulation and in association with *gata2a, cpa5* and *jun* downregulation [63–65]. Differentially expressed gene *hint1* was identified to interact with the *microphthalmia-associated transcription factor* (*MITF*) in yeast, unravelling a potential role in mast cell activation [74]. Additionally, expression of *gata2a* and *cpa5* is associated with zebrafish mast cell development and activation [65,75,76]. Finally, members of the *jun* family are recognized for their role in modulating the inflammatory response in allergy [64]. The multi-omics approach showed a shift in the transcriptome and proteome gut profile of the zebrafish treated with tick saliva towards the diminishing of pathways related with adrenergic signalling in cardiomyocytes, as well as heart and muscle contraction. In fact, the interconnection between heart and gut has been studied in both humans and zebrafish, highlighting the impact of intestinal molecules on heart physiology [77–79]. Moreover, the suppression of cardiac pathways is correlated with anaphylactic cardiovascular events [68,80]. In such cases, the decrease in cardiac output caused by systemic vasodilation, associated with the lack of smooth muscle contraction (also downregulated in treatment group transcriptome), can result in cardiac collapse and subsequently death [81,82].

Approximately 47% of human orthologous genes have a one-to-one highly concordant relationship with a zebrafish orthologue [83]. For this reason, this small teleost has been instrumental in unravelling the intricate biological activity of genes related to several human diseases [84–86]. The successful utilization of zebrafish allows for valid interspecies comparisons, which in this study revealed that supressed gut orthologous genes and proteins were mostly associated with human diseases from nervous, musculoskeletal, and cardiovascular systems, as well as nutritional/metabolic disorders. Since the gut microbiome acts as an integral part of the gastrointestinal tract, we hypothesize that tick saliva injection could have led to gut molecular modulation due to the microbiota potential implication in the development of neurological [87] and cardiovascular diseases [88,89], as well as metabolic disorders [90].

Although further in-depth metagenomics among other studies are needed to confirm these results, in this study we found that significantly suppressed pathways were involved in fatty acid metabolism and inhibition of cardiac muscle contraction, which may be associated with changes in behavior and feeding patterns. Fatty acids are integral components of lipids and are involved in the regulation of intracellular signalling pathways, transcription factor activity, and gene expression with impact on health, well-being, and disease risk [91]. In agreement with these results, Steinke et al. [92] found that the most dysregulated pathways in patients with AGS following meat challenge were involved in lipid and fatty acid metabolism, which may affect nutrient absorption and microbiome composition. These results suggest a similar response to tick saliva-induced anti-Gal IgE and meat consumption in zebrafish, thus providing additional support for this model to study AGS-related mechanisms.

Data validation of gene expression and protein representation also allowed to identify potential valuable disease biomarkers related with tick saliva allergies. Firstly, the increased genetic marker cathepsin S, associated with the zebrafish immune system, has been related to human allergic inflammation, particularly in the progression of asthma pathology [93,94]. Secondly, the downregulated gene *prkdc* is also involved in the regulation of the innate immune response and proinflammatory signaling pathways of allergies such as asthma [95]. Thirdly, *vwf* is linked to endothelial dysfunction [96], a phenomenon leading to vascular hyper-permeability in anaphylaxis [97]. Additionally, the inhibition of *acta2* may have an impact on the contraction of vascular smooth muscle cells, which play a crucial role in regulating blood flow and facilitating the healing process of damaged blood vessels [98,99]. Lastly, the underrepresented protein 60 kDa chaperonin is an immunoregulatory molecule in zebrafish and humans, that exhibits relationship with cardiovascular disease pathophysiology [100]. Diagnosis of AGS could possibly be enhanced by combining the analysis of two or more of the abovementioned potential biomarkers alongside with the standard diagnostic tools.

This study poses some limitations that should be acknowledged when interpreting the results. Although animal models are a fundamental tool when studying human diseases, it is important to recognize their limitations [101]. To provide additional support to our findings, further studies focusing on the target specie will be required. For example, although results suggest a role for α-Gal in this process, further studies on pathways identified by integrated multi-omics data that are associated with cardiomyocytes, muscle and cardiac muscle contraction are required to conclude if zebrafish are affected and/or dying from toxic shock after tick saliva injection and dog food feeding or by allergic reaction. These studies should include metagenomics, lipidomics and proteomics analysis in zebrafish treated with tick saliva and deglycosylated saliva fraction. Additionally, further experiments are required to identify cell types involved in the differential regulation of key transcripts and proteins that are critical for their tick-saliva induced phenotype. Furthermore, it is crucial to consider the small sample size used in this experiment, as it may result in limited statistical power to obtain significant results and could potentially also misrepresent the studied population. It is also important to contemplate that tick saliva intradermal administration may not fully mimic tick feeding and attachment, thus not affecting as many immunity pathways as expected

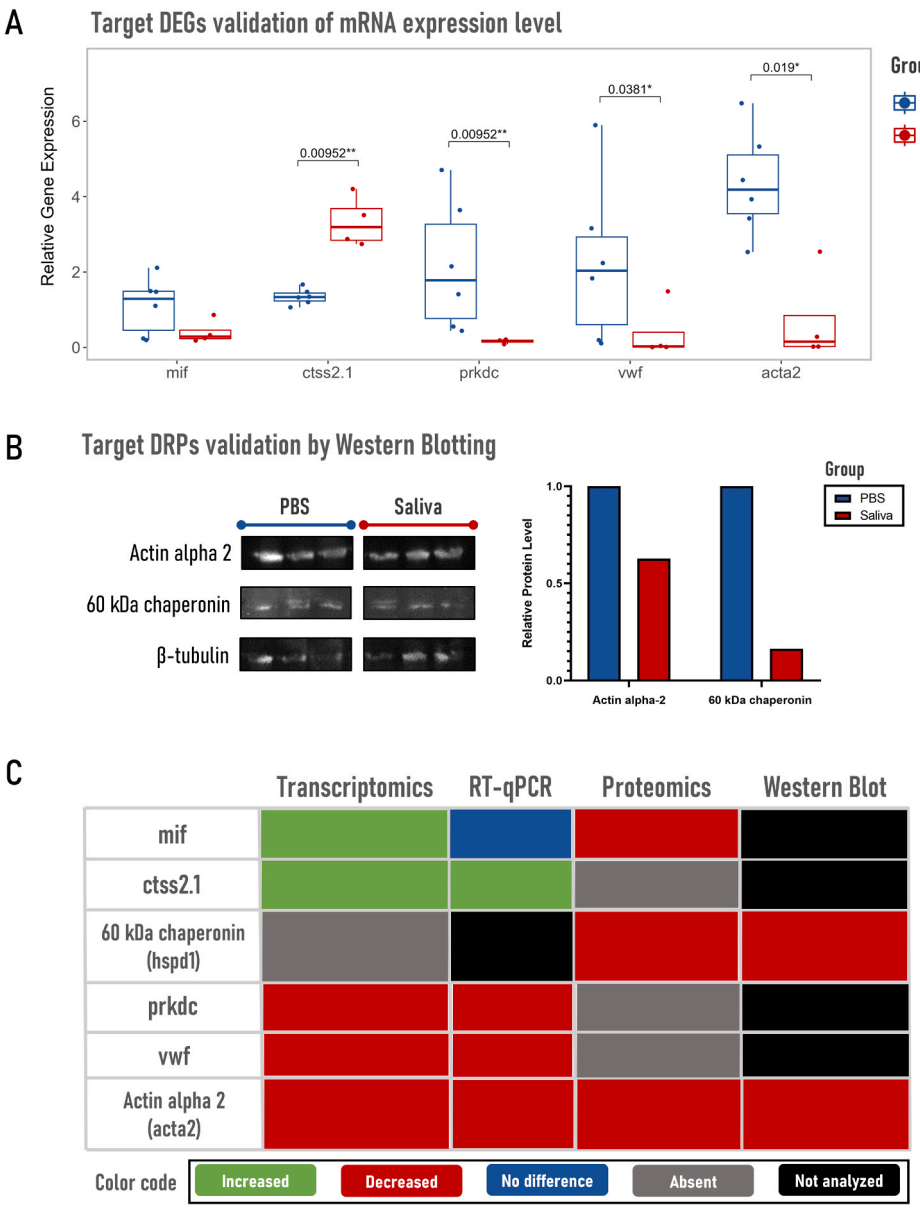

Fig. 5. Validation of mRNA levels for target differentially expressed genes (DEGs) and corroboration of target differentially represented proteins (DRPs) levels, followed by summary of target results across all methods. (A) Quantification by reverse transcriptase quantitative PCR (RT-qPCR) of changes in mRNA levels of 5 target DEGs, including the 2 upregulated genes *macrophage migration inhibitory factor (mif)* and *cathepsin S (ctss2.1)*, and 3 downregulated ones, namely *DNA-dependent protein kinase* (*prkdc*), *von Willebrand factor (vwf)* and *smooth muscle alpha-actin (acta2)*. (B) Reliability of proteomics data was confirmed by Western blotting using antibodies against target DRPs, actin alpha 2 [UniProt ID: Q6DHS1] and 60 kDa chaperonin [UniProt ID: Q803B0] and the loading control β-tubulin. (C) Analyzed targets are represented by a color code based on fold change values and according to the applied methodology.

[2]. Moreover, AGS extremely variable symptomatology [20] combined with the use of a complex pipeline methodology makes data interpretation even more intricate.

Nevertheless, the incorporation of integrated testing applying different technologies increases the robustness of results and effectively addresses some potential weaknesses. Moreover, the utilization of an integrative multi-omics strategy, focusing on transcriptomic and proteomic data, provided valuable insights into the biochemistry and dynamics of complex biological systems that underwent tick saliva inoculation followed by feeding on mammalian meat. This approach allowed to uncover crucial components in signaling pathways and aid in the discovery of novel potential biotargets for AGS diagnosis, prevention and control.

5. Conclusions

Overall, this study describes potential pathways and molecules that may play a role in the behavior and clinical signs observed in zebrafish injected with tick saliva and then fed on mammal meat. The higher presence of hemorrhagic allergic reactions, changes in behavior and feeding patterns translated into significant suppression of pathways related to cardiovascular function, behavior, sensory perception, and immune system response. Furthermore, association of supressed gut orthologous genes and proteins with nervous, musculoskeletal, cardiovascular and metabolic human diseases highlighted the potential role of α-Gal sensitization with the development or progression of certain diseases beyond the immediate AGS symptomatology. Understanding these connections is crucial for understanding the broader implications and potential long-term effects of α-Gal sensitization on overall health. These

findings may contribute to filling the knowledge gaps surrounding AGS-related biological pathways, reinforcing the multisystemic organ involvement and linking α-Gal sensitization with other illnesses. Further research in this area is required to enhance our understanding of AGS and facilitate the development of preventive and therapeutic strategies to mitigate its impact on human health.

Author statement

The authors declare that the work described has not been published previously, that it is not under consideration for publication elsewhere, and that its publication is approved by all authors.

Ethical statement

Experiments were conducted in strict accordance with the recommendations of the European Guide for the Care and Use of Laboratory Animals. Zebrafish were housed and experiments conducted at experimental facility (IREC, Ciudad Real, Spain) with the approval and supervision of the Ethics Committee on Animal Experimentation of the University of Castilla La Mancha (PR-2021–09–14) and the Counseling of Agriculture, Environment and Rural Development of Castilla La Mancha (REGA code ES130340000218). *I. ricinus* ticks were obtained from the laboratory colony maintained at the Institute of Parasitology, Biology Centre of the Czech Academy of Sciences of the Czech Republic (IPBCAS), in České Budějovice. Semi-engorged female ticks fed for 6–7 days on guinea pigs were treated with pilocarpine hydrochloride (Sigma-Aldrich, St. Louis, USA) and saliva was collected as previously described [29,41]. These animal experiments were performed in accordance with the Animal Protection Law of the Czech Republic No. 246/1992 Sb (ethics approval No. 34/2018).

CRediT authorship contribution statement

R. Vaz-Rodrigues: Data curation, Software, Methodology, Formal analysis, Writing – original draft preparation. **L. Mazuecos:** Validation, Methodology, Writing – review & editing. **M. Villar:** Conceptualization, Data curation, Resources, Methodology, Investigation, Writing – review & editing. **M. Contreras:** Methodology, Investigation, Writing – review & editing. **S. Artigas-Jerónimo:** Methodology, Investigation, Writing – review & editing. **A. González-García:** Methodology, Investigation. **C. Gortázar:** Conceptualization, Writing – review & editing. **J. de la Fuente:** Conceptualization, Resources, Supervision, Formal analysis, Project administration, Funding acquisition, Writing – review & editing.

Declaration of Competing Interest

The authors declare that the research was conducted in the absence of any commercial or financial relationships that could be construed as a potential conflict of interest.

Data Availability

All data associated with this study are included in the paper or Supplementary Materials. Transcriptomics data was deposited in the NCBI Gene Expression Omnibus (GEO) database, under the GEO series accession no. GSE237627. Proteomics data was deposited in the ProteomeXchange Consortium via the PRIDE [102] partner repository with the dataset identifier PXD043753 and 10.6019/PXD043753.

Acknowledgements

This work was supported by Ministerio de Ciencia e Innovación/ Agencia Estatal de Investigación MCIN/AEI/ 10.13039/501100011033, Spain and EU-FEDER [grant BIOGAL PID2020116761GB-I00]. R. Vaz-Rodrigues was funded by Universidad de Castilla-La Mancha (UCLM), Spain and the European Social Fund (ESF) [doctoral contract 2022-PRED-20675]. L. Mazuecos was supported by UCLM co-financed by ESF [post-doctoral grant 2021-POST-32002]. M. Contreras was funded by Ministerio de Ciencia, Innovación y Universidades, Spain [post-doctoral grant IJC2020-042710-I]. We thank David Fernández (SaBio, IREC, Spain) for his support with zebrafish facility.

Appendix A. Supporting information

Supplementary data associated with this article can be found in the online version at doi:10.1016/j.biopha.2023.115829.

References

[1] L. Šimo, M. Kazimirova, J. Richardson, S.I. Bonnet, The essential role of tick salivary glands and saliva in tick feeding and pathogen transmission, Front. Cell. Infect. Microbiol. 7 (2017) 281, https://doi.org/10.3389/fcimb.2017.00281.
[2] S.K. Wikel, Ticks and tick-borne infections: complex ecology, agents, and host interactions, Vet. Sci. 5 (2018) 60, https://doi.org/10.3390/vetsci5020060.
[3] J. Kotál, H. Langhansová, J. Lieskovská, J.F. Andersen, I.M.B. Francischetti, T. Chavakis, et al., Modulation of host immunity by tick saliva, J. Proteom. 128 (2015) 58–68, https://doi.org/10.1016/j.jprot.2015.07.005.
[4] S.R. Sharma, S. Karim, Tick saliva and the alpha-gal syndrome: finding a needle in a haystack, Front Cell Infect. Microbiol 11 (2021), 680264, https://doi.org/10.3389/fcimb.2021.680264.
[5] R. Vaz-Rodrigues, L. Mazuecos, J. de la Fuente, Current and future strategies for the diagnosis and treatment of the alpha-gal syndrome (AGS), JAA 15 (2022) 957–970, https://doi.org/10.2147/JAA.S265660.
[6] S.P. Commins, S.M. Satinover, J. Hosen, J. Mozena, L. Borish, B.D. Lewis, et al., Delayed anaphylaxis, angioedema, or urticaria after consumption of red meat in patients with IgE antibodies specific for galactose-α-1,3-galactose, 426-433.e2, J. Allergy Clin. Immunol. 123 (2009), https://doi.org/10.1016/j.jaci.2008.10.052.
[7] E. Çelebioğlu, A. Akarsu, Ü.M. Şahiner, IgE-mediated food allergy throughout life, Turk. J. Med Sci. 51 (2021) 49–60, https://doi.org/10.3906/sag-2006-95.
[8] C. Hilger, J. Fischer, F. Wölbing, T. Biedermann, Role and mechanism of galactose-alpha-1,3-galactose in the elicitation of delayed anaphylactic reactions to red meat, Curr. Allergy Asthma Rep. 19 (2019) 3, https://doi.org/10.1007/s11882-019-0835-9.
[9] M. Hils, F. Wölbing, C. Hilger, J. Fischer, N. Hoffard, T. Biedermann, The history of carbohydrates in type I allergy, Front Immunol. 11 (2020), 586924, https://doi.org/10.3389/fimmu.2020.586924.
[10] U. Galili, Evolution in primates by "Catastrophic-selection" interplay between enveloped virus epidemics, mutated genes of enzymes synthesizing carbohydrate antigens, and natural anti-carbohydrate antibodies, Am. J. Phys. Anthr. 168 (2019) 352–363, https://doi.org/10.1002/ajpa.23745.
[11] L. Mateos-Hernández, V. Risco-Castillo, E. Torres-Maravilla, L.G. Bermúdez-Humarán, P. Alberdi, A. Hodžić, et al., Gut microbiota abrogates Anti-α-Gal IgA response in lungs and protects against experimental aspergillus infection in poultry, Vaccines 8 (2020) 285, https://doi.org/10.3390/vaccines8020285.
[12] J. de la Fuente, I. Pacheco, M. Villar, A. Cabezas-Cruz, The alpha-Gal syndrome: new insights into the tick-host conflict and cooperation, Parasites Vectors 12 (2019) 154, https://doi.org/10.1186/s13071-019-3413-z.
[13] A. Cabezas-Cruz, L. Mateos-Hernández, J. Chmelař, M. Villar, J. de la Fuente, Salivary prostaglandin E2: role in tick-induced allergy to red meat, Trends Parasitol. 33 (2017) 495–498, https://doi.org/10.1016/j.pt.2017.03.004.
[14] A. Cabezas-Cruz, A. Hodžić, L. Mateos-Hernández, M. Contreras, J. de la Fuente, Tick–human interactions: from allergic klendusity to the α-Gal syndrome, Biochem. J. 478 (2021) 1783–1794, https://doi.org/10.1042/BCJ20200915.
[15] J.M. Wilson, A.J. Schuyler, N. Schroeder, T.A.E. Platts-Mills, Galactose-α-1,3-galactose: atypical food allergen or model IgE hypersensitivity? Curr. Allergy Asthma Rep. 17 (2017) 8, https://doi.org/10.1007/s11882-017-0672-7.
[16] X.L. Wong, D.F. Sebaratnam, Mammalian meat allergy, Int J. Dermatol. 57 (2018) 1433–1436, https://doi.org/10.1111/ijd.14208.
[17] I. Young, C. Prematunge, K. Pussegoda, T. Corrin, L. Waddell, Tick exposures and alpha-gal syndrome: a systematic review of the evidence, Ticks Tick. -Borne Dis. 12 (2021), 101674, https://doi.org/10.1016/j.ttbdis.2021.101674.
[18] S. van Nunen, Tick-induced allergies: mammalian meat allergy, tick anaphylaxis and their significance, Asia Pac. Allergy 5 (2015) 3, https://doi.org/10.5415/apallergy.2015.5.1.3.
[19] T.A.E. Platts-Mills, S.P. Commins, T. Biedermann, M. van Hage, M. Levin, L. A. Beck, et al., On the cause and consequences of IgE to galactose-α-1,3-galactose: a report from the national institute of allergy and infectious diseases workshop on understanding IgE-mediated mammalian meat allergy, J. Allergy Clin. Immunol. 145 (2020) 1061–1071, https://doi.org/10.1016/j.jaci.2020.01.047.
[20] J.D. Macdougall, K.O. Thomas, O.I. Iweala, The meat of the matter: understanding and managing alpha-gal syndrome, ITT Volume 11 (2022) 37–54, https://doi.org/10.2147/ITT.S276872.
[21] J.M. Wilson, A.T. Nguyen, A.J. Schuyler, S.P. Commins, A.M. Taylor, T.A. E. Platts-Mills, et al., IgE to the mammalian oligosaccharide galactose-α-1,3-galactose is associated with increased atheroma volume and plaques with

unstable characteristics-brief report, Arterioscler. Thromb. Vasc. Biol. 38 (2018) 1665–1669, https://doi.org/10.1161/ATVBAHA.118.311222.
[22] J.M. Wilson, C.A. McNamara, T.A.E. Platts-Mills, IgE, α-Gal and atherosclerosis, Aging (Albany NY) 11 (2019) 1900–1902, https://doi.org/10.18632/aging.101894.
[23] B. Daripa, S. Lucchese, Novel case presentation of abulia after lone star tick bite as evidenced by raised titers of alpha-gal specific IgM immunoglobulin and a possibility of alpha-gal driven hypothalamic dysfunction as the pathomechanism, Cureus 14 (2022), e24551, https://doi.org/10.7759/cureus.24551.
[24] H. Can, S.K. Chanumolu, E. Gonzalez-Muñoz, S. Prukudom, H.H. Otu, J.B. Cibelli, Comparative analysis of single-cell transcriptomics in human and zebrafish oocytes, BMC Genom. 21 (2020) 471, https://doi.org/10.1186/s12864-020-06860-z.
[25] T. Teame, Z. Zhang, C. Ran, H. Zhang, Y. Yang, Q. Ding, et al., The use of zebrafish (Danio rerio) as biomedical models, Anim. Front 9 (2019) 68–77, https://doi.org/10.1093/af/vfz020.
[26] R.L. Bailone, H.C.S. Fukushima, B.H. Ventura Fernandes, L.K. De Aguiar, T. Corrêa, H. Janke, et al., Zebrafish as an alternative animal model in human and animal vaccination research, Lab Anim. Res. 36 (2020) 13, https://doi.org/10.1186/s42826-020-00042-4.
[27] F. Progatzky, H.T. Cook, J.R. Lamb, L. Bugeon, M.J. Dallman, Mucosal inflammation at the respiratory interface: a zebrafish model, Am. J. Physiol. -Lung Cell. Mol. Physiol. 310 (2016) L551–L561, https://doi.org/10.1152/ajplung.00323.2015.
[28] F. Progatzky, A. Jha, M. Wane, R.S. Thwaites, S. Makris, R.J. Shattock, et al., Induction of innate cytokine responses by respiratory mucosal challenge with R848 in zebrafish, mice, and humans, 342-345.e7, J. Allergy Clin. Immunol. 144 (2019), https://doi.org/10.1016/j.jaci.2019.04.003.
[29] M. Contreras, I. Pacheco, P. Alberdi, S. Díaz-Sánchez, S. Artigas-Jerónimo, L. Mateos-Hernández, et al., Allergic reactions and immunity in response to tick salivary biogenic substances and red meat consumption in the zebrafish model, Front Cell Infect. Microbiol 10 (2020) 78, https://doi.org/10.3389/fcimb.2020.00078.
[30] M. Contreras, A. González-García, J. de la Fuente, Zebrafish animal model for the study of allergic reactions in response to tick saliva biomolecules, J. Vis. Exp. (2022), https://doi.org/10.3791/64378.
[31] M. Contreras, R. Vaz-Rodrigues, L. Mazuecos, M. Villar, S. Artigas-Jerónimo, A. González-García, et al., Allergic reactions to tick saliva components in zebrafish model, Parasites Vectors 16 (2023) 242, https://doi.org/10.1186/s13071-023-05874-2.
[32] N.D. Lawson, R. Li, M. Shin, A. Grosse, O. Yukselen, O.A. Stone, et al., An improved zebrafish transcriptome annotation for sensitive and comprehensive detection of cell type-specific genes, eLife 9 (2020), e55792, https://doi.org/10.7554/eLife.55792.
[33] T.-Y. Choi, T.-I. Choi, Y.-R. Lee, S.-K. Choe, C.-H. Kim, Zebrafish as an animal model for biomedical research, Exp. Mol. Med. 53 (2021) 310–317, https://doi.org/10.1038/s12276-021-00571-5.
[34] D.S. Kelkar, E. Provost, R. Chaerkady, B. Muthusamy, S.S. Manda, T. Subbannayya, et al., Annotation of the zebrafish genome through an integrated transcriptomic and proteomic analysis, Mol. Cell. Proteom. 13 (2014) 3184–3198, https://doi.org/10.1074/mcp.M114.038299.
[35] M. Villar, N. Ayllón, P. Alberdi, A. Moreno, M. Moreno, R. Tobes, et al., Integrated metabolomics, transcriptomics and proteomics identifies metabolic pathways affected by anaplasma phagocytophilum infection in tick cells, Mol. Cell. Proteom. 14 (2015) 3154–3172, https://doi.org/10.1074/mcp.M115.051938.
[36] M. Villar, I. Pacheco, L. Mateos-Hernández, A. Cabezas-Cruz, A.E. Tabor, M. Rodríguez-Valle, et al., Characterization of tick salivary gland and saliva alphagalactome reveals candidate alpha-gal syndrome disease biomarkers, Expert Rev. Prote 18 (2021) 1099–1116, https://doi.org/10.1080/14789450.2021.2018305.
[37] E. Cheung, D. Chatterjee, R. Gerlai, Subcutaneous dye injection for marking and identification of individual adult zebrafish (Danio rerio) in behavioral studies, Behav. Res 46 (2014) 619–624, https://doi.org/10.3758/s13428-013-0399-x.
[38] Vasavada N. Online Web Statistical Calculators 2016. ⟨https://astatsa.com/⟩ (accessed October 24, 2022).
[39] I. Pacheco, M. Contreras, M. Villar, M.A. Risalde, P. Alberdi, A. Cabezas-Cruz, et al., Vaccination with alpha-gal protects against mycobacterial infection in the zebrafish model of tuberculosis, Vaccines 8 (2020) 195, https://doi.org/10.3390/vaccines8020195.
[40] A. Mesika, G. Nadav, C. Shochat, L. Kalfon, K. Jackson, A. Khalaileh, et al., NGLY1 deficiency zebrafish model manifests abnormalities of the nervous and musculoskeletal systems, Front. Cell Dev. Biol. (2022) 10, https://doi.org/10.3389/fcell.2022.902969.
[41] K. Kýčková, J. Kopecký, Effect of tick saliva on mechanisms of innate immune response against borrelia afzelii, J. Med. Entomol. 43 (2006) 1208–1214, https://doi.org/10.1093/jmedent/43.6.1208.
[42] Andrews S. FastQC: A Quality Control Tool for High Throughput Sequence Data 2010.
[43] T. Smith, A. Heger, I. Sudbery, UMI-tools: modeling sequencing errors in Unique Molecular Identifiers to improve quantification accuracy, Genome Res 27 (2017) 491–499, https://doi.org/10.1101/gr.209601.116.
[44] M. Martin, Cutadapt removes adapter sequences from high-throughput sequencing reads, EMBnetJournal 17 (2011) 10–12, https://doi.org/10.14806/ej.17.1.200.
[45] A. Dobin, C.A. Davis, F. Schlesinger, J. Drenkow, C. Zaleski, S. Jha, et al., STAR: ultrafast universal RNA-seq aligner, Bioinformatics 29 (2013) 15–21, https://doi.org/10.1093/bioinformatics/bts635.
[46] Y. Liao, G.K. Smyth, W. Shi, featureCounts: an efficient general purpose program for assigning sequence reads to genomic features, Bioinformatics 30 (2014) 923–930, https://doi.org/10.1093/bioinformatics/btt656.
[47] M.I. Love, W. Huber, S. Anders, Moderated estimation of fold change and dispersion for RNA-seq data with DESeq2, Genome Biol. 15 (2014) 550, https://doi.org/10.1186/s13059-014-0550-8.
[48] R Core Team. R: The R Project for Statistical Computing 2023.
[49] Z. Gu, Complex heatmap visualization, iMeta 1 (2022), e43, https://doi.org/10.1002/imt2.43.
[50] Blighe K., Rana S., Lewis M. EnhancedVolcano: Publication-ready volcano plots with enhanced colouring and labeling 2022.
[51] M. Villar, J.M. Urra, F.J. Rodríguez-del-Río, S. Artigas-Jerónimo, N. Jiménez-Collados, E. Ferreras-Colino, et al., Characterization by quantitative serum proteomics of immune-related prognostic biomarkers for COVID-19 symptomatology, Front. Immunol. (2021) 12, https://doi.org/10.3389/fimmu.2021.730710.
[52] T. Wu, E. Hu, S. Xu, M. Chen, P. Guo, Z. Dai, et al., clusterProfiler 4.0: a universal enrichment tool for interpreting omics data, Innov. (Camb.) 2 (2021), 100141, https://doi.org/10.1016/j.xinn.2021.100141.
[53] G. Yu, L.-G. Wang, Y. Han, Q.-Y. He, clusterProfiler: an R package for comparing biological themes among gene clusters, OMICS 16 (2012) 284–287, https://doi.org/10.1089/omi.2011.0118.
[54] G. Yu, L.-G. Wang, G.-R. Yan, Q.-Y. He, DOSE: an R/Bioconductor package for disease ontology semantic and enrichment analysis, Bioinformatics 31 (2015) 608–609, https://doi.org/10.1093/bioinformatics/btu684.
[55] Carlson M. org.Dr.eg.db: Genome wide annotation for Zebrafish 2022.
[56] Yu G. enrichplot: Visualization of Functional Enrichment Result 2022.
[57] Schilder B.M., Skene N.G. orthogene: Interspecies gene mapping 2022.
[58] J. Piñero, J.M. Ramírez-Anguita, J. Saüch-Pitarch, F. Ronzano, E. Centeno, F. Sanz, et al., The DisGeNET knowledge platform for disease genomics: 2019 update, Nucleic Acids Res. 48 (2020) D845–D855, https://doi.org/10.1093/nar/gkz1021.
[59] S. Canzler, J. Hackermüller, multiGSEA: a GSEA-based pathway enrichment analysis for multi-omics data, BMC Bioinforma. 21 (2020) 561, https://doi.org/10.1186/s12859-020-03910-x.
[60] J. Ye, G. Coulouris, I. Zaretskaya, I. Cutcutache, S. Rozen, T.L. Madden, Primer-BLAST: a tool to design target-specific primers for polymerase chain reaction, BMC Bioinforma. 13 (2012) 134, https://doi.org/10.1186/1471-2105-13-134.
[61] J. Hellemans, G. Mortier, A. De Paepe, F. Speleman, J. Vandesompele, qBase relative quantification framework and software for management and automated analysis of real-time quantitative PCR data, Genome Biol. 8 (2007) R19, https://doi.org/10.1186/gb-2007-8-2-r19.
[62] J. Vandesompele, K. De Preter, F. Pattyn, B. Poppe, N. Van Roy, A. De Paepe, et al., Accurate normalization of real-time quantitative RT-PCR data by geometric averaging of multiple internal control genes, Genome Biol. 3 (2002) research0034.1-research0034.11.
[63] M. Dillenburg, J. Smith, C.R. Wagner, The many faces of histidine triad nucleotide binding protein 1 (HINT1), ACS Pharm. Transl. Sci. 6 (2023) 1310–1322, https://doi.org/10.1021/acsptsci.3c00079.
[64] L. Escoubet-Lozach, C.K. Glass, S.I. Wasserman, The role of transcription factors in allergic inflammation, J. Allergy Clin. Immunol. 110 (2002) 553–564, https://doi.org/10.1067/mai.2002.128076.
[65] S.I. Da'as, A.J. Coombs, T.B. Balci, C.A. Grondin, A.A. Ferrando, J.N. Berman, The zebrafish reveals dependence of the mast cell lineage on Notch signaling in vivo, Blood 119 (2012) 3585–3594, https://doi.org/10.1182/blood-2011-10-385989.
[66] X. Zhao, Y. Liu, J. Xie, L. Zhang, Q. Zhu, L. Su, et al., The manipulation of cell suspensions from zebrafish intestinal mucosa contributes to understanding enteritis, Front Immunol. 14 (2023), 1193977, https://doi.org/10.3389/fimmu.2023.1193977.
[67] N. Bernabò, A. Ordinelli, R. Di Agostino, M. Mattioli, B. Barboni, Network analyses of sperm–egg recognition and binding: ready to rethink fertility mechanisms? OMICS 18 (2014) 740–753, https://doi.org/10.1089/omi.2014.0128.
[68] M. Triggiani, V. Patella, R.I. Staiano, F. Granata, G. Marone, Allergy and the cardiovascular system, Clin. Exp. Immunol. 153 (2008) 7–11, https://doi.org/10.1111/j.1365-2249.2008.03714.x.
[69] K. Bergmann, G. Sypniewska, Is there an association of allergy and cardiovascular disease? Biochem Med (2011) 210–218, https://doi.org/10.11613/BM.2011.030.
[70] A. Cabezas-Cruz, J.J. Valdés, Are ticks venomous animals? Front Zool. 11 (2014) 47, https://doi.org/10.1186/1742-9994-11-47.
[71] J. Guo, Y. Zhang, T. Liu, B.D. Levy, P. Libby, G.-P. Shi, Allergic asthma is a risk factor for human cardiovascular diseases, Nat. Cardiovasc Res 1 (2022) 417–430, https://doi.org/10.1038/s44161-022-00067-z.
[72] J.W. Steinke, T.A.E. Platts-Mills, S.P. Commins, The alpha-gal story: lessons learned from connecting the dots, J. Allergy Clin. Immunol. 135 (2015) 589–596, https://doi.org/10.1016/j.jaci.2014.12.1947.
[73] M.G. Flaherty, S.J. Kaplan, M.R. Jerath, Diagnosis of life-threatening alpha-gal food allergy appears to be patient driven, J. Prim. Care Community Health 8 (2017) 345–348, https://doi.org/10.1177/2150131917705714.
[74] E. Razin, Z.C. Zhang, H. Nechushtan, S. Frenkel, Y.-N. Lee, R. Arudchandran, et al., Suppression of microphthalmia transcriptional activity by its association with protein kinase C-interacting protein 1 in mast cells*, J. Biol. Chem. 274 (1999) 34272–34276, https://doi.org/10.1074/jbc.274.48.34272.

[75] S.I. Da'as, T.B. Balci, J.N. Berman, Mast cell development and function in the zebrafish, Methods Mol. Biol. 1220 (2015) 29–57, https://doi.org/10.1007/978-1-4939-1568-2_3.
[76] J.T. Dobson, J. Seibert, E.M. Teh, S. Da'as, R.B. Fraser, B.H. Paw, et al., Carboxypeptidase A5 identifies a novel mast cell lineage in the zebrafish providing new insight into mast cell fate determination, Blood 112 (2008) 2969–2972, https://doi.org/10.1182/blood-2008-03-145011.
[77] G. Rogler, G. Rosano, The heart and the gut, Eur. Heart J. 35 (2014) 426–430, https://doi.org/10.1093/eurheartj/eht271.
[78] K.V.C. Reddy, Heart-gut axis: targeting proprotein convertase subtilisin/kexin type 9 (PCSK9) to prevent cardiovascular disease through gut microbiota, Med. Microecol. 7 (2021), 100033, https://doi.org/10.1016/j.medmic.2021.100033.
[79] H. Sree Kumar, A.S. Wisner, J.M. Refsnider, C.J. Martyniuk, J. Zubcevic, Small fish, big discoveries: zebrafish shed light on microbial biomarkers for neuro-immune-cardiovascular health, Front. Physiol. (2023) 14.
[80] N.G. Kounis, G.D. Soufras, G. Hahalis, Anaphylactic shock: kounis hypersensitivity-associated syndrome seems to be the primary cause, N. Am. J. Med Sci. 5 (2013) 631–636, https://doi.org/10.4103/1947-2714.122304.
[81] N.G. Kounis, G. Cervellin, I. Koniari, L. Bonfanti, P. Dousdampanis, N. Charokopos, et al., Anaphylactic cardiovascular collapse and Kounis syndrome: systemic vasodilation or coronary vasoconstriction? Ann. Transl. Med 6 (2018) 332, https://doi.org/10.21037/atm.2018.09.05.
[82] M. Ruiz-Garcia, J. Bartra, O. Alvarez, A. Lakhani, S. Patel, A. Tang, et al., Cardiovascular changes during peanut-induced allergic reactions in human subjects, J. Allergy Clin. Immunol. 147 (2021) 633–642, https://doi.org/10.1016/j.jaci.2020.06.033.
[83] K. Howe, M.D. Clark, C.F. Torroja, J. Torrance, C. Berthelot, M. Muffato, et al., The zebrafish reference genome sequence and its relationship to the human genome, Nature 496 (2013) 498–503, https://doi.org/10.1038/nature12111.
[84] J. García-González, B. de Quadros, W. Havelange, A.J. Brock, C.H. Brennan, Behavioral effects of developmental exposure to JWH-018 in wild-type and disrupted in schizophrenia 1 (disc1) mutant zebrafish, Biomolecules 11 (2021) 319, https://doi.org/10.3390/biom11020319.
[85] M. Breuer, S.A. Patten, A great catch for investigating inborn errors of metabolism—insights obtained from zebrafish, Biomolecules 10 (2020) 1352, https://doi.org/10.3390/biom10091352.
[86] C. Golzio, J. Willer, M.E. Talkowski, E.C. Oh, Y. Taniguchi, S. Jacquemont, et al., KCTD13 is a major driver of mirrored neuroanatomical phenotypes of the 16p11.2 copy number variant, Nature 485 (2012) 363–367, https://doi.org/10.1038/nature11091.
[87] K. Suganya, B.-S. Koo, Gut–brain axis: role of gut microbiota on neurological disorders and how probiotics/prebiotics beneficially modulate microbial and immune pathways to improve brain functions, Int J. Mol. Sci. 21 (2020) 7551, https://doi.org/10.3390/ijms21207551.
[88] M. Jin, Z. Qian, J. Yin, W. Xu, X. Zhou, The role of intestinal microbiota in cardiovascular disease, J. Cell Mol. Med 23 (2019) 2343–2350, https://doi.org/10.1111/jcmm.14195.
[89] Md.M. Rahman, F. Islam, Md.H. -Or-Rashid, A.A. Mamun, Md.S. Rahaman, M.D. M. Islam, et al., The gut microbiota (microbiome) in cardiovascular disease and its therapeutic regulation, Front. Cell. Infect. Microbiol. (2022) 12.
[90] K.Y. Hur, M.-S. Lee, Gut microbiota and metabolic disorders, Diabetes Metab. J. 39 (2015) 198–203, https://doi.org/10.4093/dmj.2015.39.3.198.
[91] P.C. Calder, Functional roles of fatty acids and their effects on human health, JPEN J. Parent. Enter. Nutr. 39 (2015) 18S–32S, https://doi.org/10.1177/0148607115595980.
[92] J.W. Steinke, S.L. Pochan, H.R. James, T.A.E. Platts-Mills, S.P. Commins, Altered metabolic profile in patients with IgE to galactose-alpha-1,3-galactose following in vivo food challenge, 1465-1467.e8, J. Allergy Clin. Immunol. 138 (2016), https://doi.org/10.1016/j.jaci.2016.05.021.
[93] V.B. Reddy, S.G. Shimada, P. Sikand, R.H. LaMotte, E.A. Lerner, Cathepsin S elicits itch and signals via protease-activated receptors, J. Invest Dermatol. 130 (2010) 1468–1470, https://doi.org/10.1038/jid.2009.430.
[94] R.D.A. Wilkinson, R. Williams, C.J. Scott, R.E. Burden, Cathepsin S: therapeutic, diagnostic, and prognostic potential, Biol. Chem. 396 (2015) 867–882, https://doi.org/10.1515/hsz-2015-0114.
[95] Y. Wang, J. Lin, J. Shu, H. Li, Z. Ren, Oxidative damage and DNA damage in lungs of an ovalbumininduced asthmatic murine model, J. Thorac. Dis. (2018) 10, https://doi.org/10.21037/jtd.2018.07.74.
[96] M. Abudoukelimu, B. Ba, Y. Kai Guo, J. Xu, Von Willebrand factor (vWF) in patients with heart failure with preserved ejection fraction (HFpEF): a retrospective observational study, Medicine 101 (2022), e29854, https://doi.org/10.1097/MD.0000000000029854.
[97] T. Nakamura, T. Murata, Regulation of vascular permeability in anaphylaxis, Br. J. Pharm. 175 (2018) 2538–2542, https://doi.org/10.1111/bph.14332.
[98] G. Cao, X. Xuan, J. Hu, R. Zhang, H. Jin, H. Dong, How vascular smooth muscle cell phenotype switching contributes to vascular disease, Cell Commun. Signal. 20 (2022) 180, https://doi.org/10.1186/s12964-022-00993-2.
[99] S.-M. Yuan, α-smooth muscle actin and ACTA2 gene expressions in vasculopathies, Braz. J. Cardiovasc Surg. 30 (2015) 644–649, https://doi.org/10.5935/1678-9741.20150081.
[100] I. Krishnan-Sivadoss, I.A. Mijares-Rojas, R.A. Villarreal-Leal, G. Torre-Amione, A. A. Knowlton, C.E. Guerrero-Beltrán, Heat shock protein 60 and cardiovascular diseases: an intricate love-hate story, Med Res Rev. 41 (2021) 29–71, https://doi.org/10.1002/med.21723.
[101] T. Hartung, Thoughts on limitations of animal models, Park. Relat. Disord. 14 (Suppl 2) (2008) S81–S83, https://doi.org/10.1016/j.parkreldis.2008.04.003.
[102] Y. Perez-Riverol, J. Bai, C. Bandla, D. García-Seisdedos, S. Hewapathirana, S. Kamatchinathan, et al., The PRIDE database resources in 2022: a hub for mass spectrometry-based proteomics evidences, Nucleic Acids Res 50 (2022) D543–D552, https://doi.org/10.1093/nar/gkab1038.